

# Design of solder joints for fundamental studies on the effects of electromigration

C. E. Ho · A. Lee · K. N. Subramanian

Received: 2 March 2007 / Accepted: 7 March 2007 / Published online: 24 March 2007  
© Springer Science+Business Media, LLC 2007

**Abstract** The continuous miniaturization of high performance electronic devices has reached a level at which current densities are large enough to make electromigration (EM) a significant issue affecting the electrical and mechanical reliability of solder joints. A new design of solder joints that controls the extent of regions experiencing relatively uniform current density, as well as regions with large current density gradient was developed. Current density distribution of this newly designed solder joint was calculated using finite element analysis (FEA), which was used to guide the characterization of EM of real solder joints. As a part of the effort in evaluating the suitability of the new joint configuration for evaluating the fundamental issues in EM, eutectic PbSn solder joints were fabricated using this design. EM effects due to applied current, current density distribution, and joint thickness of eutectic PbSn solder joints present in this joint configuration were investigated. Findings based on this new design can facilitate fundamental studies of EM issues that affect the reliability of solder joints.

## 1 Introduction

Due to the miniaturization of modern microelectronics, solder joints can easily experience current densities more than  $10^3$  Amp/cm<sup>2</sup> [1]. Under such conditions, electromigration (EM) becomes a serious reliability concern for

electronic packaging. EM is movement of the conducting materials due to interactions between conducting electrons and diffusing metal atoms/ions. To understand fundamentals of these complex interactions, and to investigate failure mechanisms in solder joints at various operating conditions, there is a need to develop an appropriate joint configuration for comparing the reliability of different solder alloys, and/or to develop mitigation strategies to combat the deleterious effects of EM. The currently popular joint configuration employed by the electronic manufacturers utilizes circuit with solder bumps. In such a configuration there exists an induced ‘‘current crowding’’ due to an extreme thin-thick divergence where local current densities can vary by two or more orders of magnitude over a very short distance [1–3]. This local high current density can lead to a significant Joule heating resulting in the local temperatures reaching much higher values than the environment [4–8]. According to the results by Ye et al. [4], the thermal gradient can reach 1500 °C/cm from the chip side to the board side, which is sufficient to induce a visible thermomigration of atoms from the board side to the chip side. In other words, in a real flip-chip joint, the movement direction of the atoms driven by thermal gradient will be along a direction opposite to that driven by electric current. In addition, the cross-interaction induced by the chemical potential between the two solder/pad interfaces could also drive the atoms of the base metal across the whole joint, where the movement of the atoms actually can also go in the opposite direction to the electric current [9]. Therefore, it is difficult to carry out studies that isolate critical events due to the EM using the currently popular solder bump configuration. To minimize the current crowding, as well as the Joule heating, modifications to the joint geometry by adjusting the current path to be straight, and more uniform, before entering the solder are being considered and adopted

---

C. E. Ho · A. Lee · K. N. Subramanian (✉)  
Department of Chemical Engineering and Materials Science,  
Michigan State University, East Lansing, MI 48824, USA  
e-mail: subraman@egr.msu.edu

by industry [10, 11]. This paper, deals with development of a new solder joint design that can be used to carry out some fundamentally critical studies on the effects of EM on solder joints in a laboratory environment. Finite element analysis (FEA) was performed to evaluate current density distribution of different joint thicknesses using a global mean current density of  $10^4$  Amp/cm<sup>2</sup>. To verify the FEA simulation, actual eutectic PbSn solder joints with dimensions similar to that used in FEA were fabricated and subjected to an electrical force with global current density of  $10^4$  Amp/cm<sup>2</sup>. This paper presents effects of current density distribution as calculated by FEA and surface features of eutectic PbSn solder joints of different thickness subjected to an electrical force with global current density of  $10^4$  Amp/cm<sup>2</sup>.

## 2 Experimental

### 2.1 Sample preparation

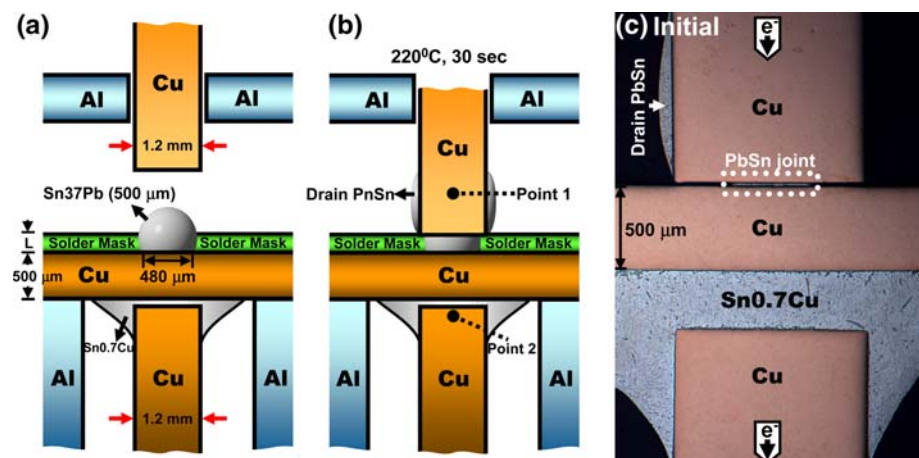
Schematics illustrating the details corresponding to the steps described in preparing the solder joints in the newly developed configuration are provided in Fig. 1. Two different solder joints,  $25(\pm 2)$   $\mu\text{m}$  and  $75(\pm 3)$   $\mu\text{m}$  in thickness, were utilized to probe the behavior of EM as influenced by the size of the joint. These thicknesses were selected based on the possible dimensions of bump height for the current or future use in the flip-chip packaging technology. They were fabricated by inserting a 1.2 mm diameter Cu pillar onto a molten eutectic PbSn bead of 500  $\mu\text{m}$  in diameter over a Cu pad with an opening of 480  $\mu\text{m}$ . Due to the different thickness of solder mask (L),  $\{18(\pm 1)$   $\mu\text{m}$  and  $68(\pm 1)$   $\mu\text{m}\}$  coating on the pads, the height of the joints can be accurately controlled. During the squeezing process, the excessive solder was drained from the pad and wetted the inserted pillar. The drained solder

remained between the pillar and the mask, as well as the dissolution of Cu during the soldering process, led to a difference of about 7  $\mu\text{m}$  between the height of joint and the thickness of mask.

Prior to the soldering, the tips of Cu pillars were metallographically polished, cleaned by nitric acid solution and water, and then fluxed. One of them was soldered on the backside of the Cu pad by using eutectic SnCu in order to conduct the electric current. The use of eutectic SnCu assured the backside of this joint will not fall off in the sequential soldering due to its higher melting point of 227 °C. The entire package, the Cu pad plus the back-side of the joint, was then placed on an aluminum stage and heated to  $220(\pm 3)$  °C. At this temperature, a fluxed 500  $\mu\text{m}$  diameter eutectic PbSn sphere was then placed between the openings of solder mask for 2 min. The topside Cu pillar shown in Fig. 1a was then inserted and squeezed for 30 s. During this inserting, another aluminum stage with a 1.28 mm-diameter hole was used to ensure vertical alignment. Schematic drawings and the actual solder joint produced by this technique are shown in Fig. 1.

In order to facilitate intermittent observations during current stressing, the joints were cross-sectioned and metallographically polished to over one-half of the joint diameter before applying electrical current. The cross-sectional drawing of the polished solder joint is shown in Fig. 2. For current stressing, a constant electrical current of 5.9 Amps was passed through the solder joints, which generated a global average current density of  $10^4$  Amp/cm<sup>2</sup> within the solder joint based on the known solder joint dimensions. Current stressing experiments were then performed in a constant temperature environment by placing the entire solder joint into a temperature-controlled, convection air oven set at the specified temperature of  $150(\pm 2)$  °C. In order to monitor the temperature gradient across the joint that can arise from Joule heating, the temperature of solder joints was monitored using a pair of

**Fig. 1** Schematic drawing showing the fabrication of the solder joint before soldering (a), and after soldering (b). (c) Optical micrograph showing the whole configuration of the as-soldered joint (25  $\mu\text{m}$  thick in PbSn joint). The symbol L represented the thickness of the solder mask, which were  $18(\pm 1)$ , and  $68(\pm 1)$   $\mu\text{m}$  respectively



k-type thermocouples with diameter of 0.4 mm attached to two locations (points 1 & 2) at equal distance away from the PbSn solder as indicated in Fig. 1b. The distance between the two points is about 2 mm. In this solder joint design, the extent of regions experiencing relatively uniform current density, as well as regions with large current density gradient can be controlled by choosing appropriate ratios Cu pillar diameter to solder diameter.

After current stressing for a known period of time, surface features of the solder joints were investigated using optical microscopy (OM) in reflection mode, and a JEOL 6400 scanning electron microscopy operated at 20 keV. The chemical composition of each phase was identified by the energy dispersive X-ray analysis (EDX). In order to quantitatively measure the surface deformation of the solder after the EM, a confocal laser scanning microscope (CLSM) (Type: Zeiss Pascal, German) in the 20/80 reflection mode was used. During the scanning, a mono-light laser with the wavelength of 488 nm (blue-light laser) was utilized to raster across the specimen in a specific focal  $x$ - $y$  plane. In order to construct a 3-dimensional contour, a series of the images in each horizontal focal plane ( $x$ - $y$  plane) was gathered individually by gradually moving the stage along the  $z$ -axis. The depth of the scanning resolution was set at 1.7  $\mu\text{m}$  per step.

## 2.2 Simulation of current density distribution

Current density distribution within the solder joint was simulated using ANSYS finite element software. In Fig. 3a, a 3-dimensional solid model with meshization of the entire Cu/solder/Cu joint is presented. Figure 3b is the expanded view of the eutectic PbSn solder disc. This solid model was meshed using the SOLID69 thermal-electric coupled field element. The SOLID69 element has eight

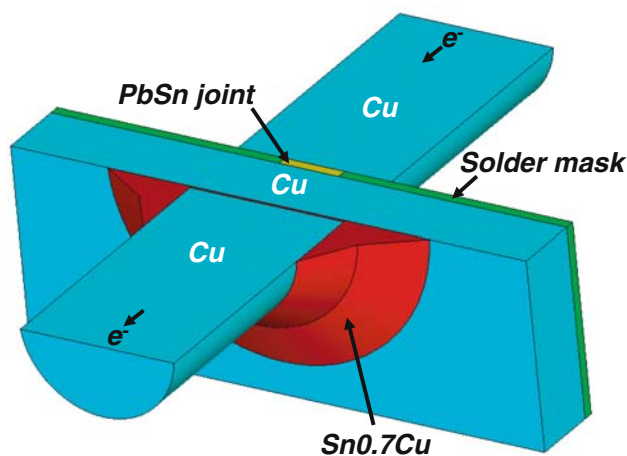


**Fig. 2** Schematic drawing showing the joint configuration used in study

nodes with two degrees of freedom, temperature and voltage, at each node. In this study, the variation of temperature due to Joule heating was ignored, and the reason for the same will be discussed later. The dimension of the meshes of eutectic PbSn was 5.0  $\mu\text{m}$  along the  $x$ -axis, as shown in Fig. 3b. In order to simplify the computations, the thickness of reaction products ( $\text{Cu}_6\text{Sn}_5$  and  $\text{Cu}_3\text{Sn}$ ) was also ignored since they were kinetically generated during the test. A current of 5.9 Amps was applied during the simulation leading to a global current density of  $10^4 \text{ Amp/cm}^2$ , as verified by the sum-average of all individual simulated elements.

## 3 Results and discussion

### 3.1 FEA simulations

Results of current density distribution of solder joints with thickness of 25  $\mu\text{m}$  and 75  $\mu\text{m}$  from the FEA simulation are shown in Figs. 4a and b, respectively. The targeted current density for studies with these joints was  $10^4 \text{ Amp/cm}^2$ . Results from the simulation showed that more than 80 volume percent of solder within the joint has current densities in-between  $\pm 15\%$  of the targeted value, regardless of the thickness of the joint. The gradient of current density becomes steeper at the outer edges of the joints. In addition, as the thickness of the joint increases, the contours of equal current density become an hour-glass shaped along the thickness direction. Hence, the steepness of current density gradient becomes much more significant as the joint thickness increases. This simulation result suggests that damages due to current crowding is to be located along the outer edges of the thickness and are more serious as the joint thickness increases.

### 3.2 Temperature measurements

The temperature across the joints was measured directly by attaching a fine-gage thermocouple to points 1 and 2, as shown in Fig. 1b, with one additional thermocouple in direct contact to the solder. During the 5.9 Amps current stressing, the temperature at all three locations raised to about  $2.5(\pm 2)^\circ\text{C}$  above the ambient environment temperatures over a range of 30–150  $^\circ\text{C}$ ; this temperature raise is referred as Joule heating. Unlike in circuit of solder bump flip-chip joints, no serious heat generation occurs in the solder present in the current configuration. Such a feature reflects two facts: (1) the current crowding in the newly designed joint should be much lower, and (2) the presence of Cu pillars and substrate (as shown in Fig. 1) facilitate effective heat dissipation. In addition, we observed no significant temperature difference between points 1 and 2.

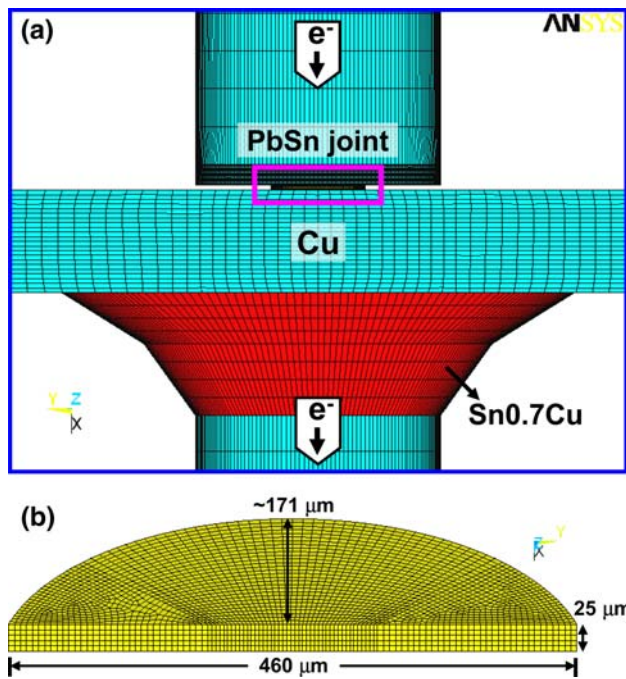


**Fig. 3** (a) Simulation model with meshization in this study. (b) Zoom-in picture of the PbSn joint in (a) (The coordinate system of b is tilted by 30°)

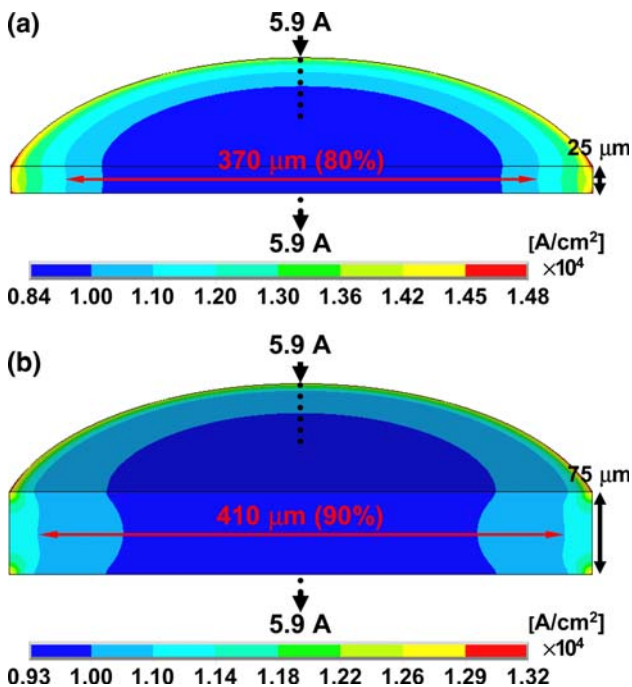


**Fig. 4** Simulation result showing the current density distribution of the PbSn joints with the thickness of 25  $\mu\text{m}$  (a), and 75  $\mu\text{m}$  (b). A 5.9 Amps current now was applied in the modes

This suggests that there was no significant thermal gradient from the cathode side to the anode side, in the joint configuration employed. These observations support the

simulation results where the current density distribution in the solder was relatively symmetrical, and the current crowding within the solder was not a significant issue, therefore the effect of thermal gradient can be ruled out in this joint design.

### 3.3 Surface features upon electrical current stressing

Microstructural features of as-jointed and polished specimens of two different thicknesses are provided in Fig. 5. Uniform microstructure consisting of inter-woven Pb-rich, and Sn-rich phases present in both joints can be noted in this figure. Figure 6a and b show the secondary electron images of the newly designed solder joints with thickness of 25  $\mu\text{m}$  and 75  $\mu\text{m}$  using eutectic PbSn after a continuous electrical current stressing of  $10^4$  Amp/cm<sup>2</sup> for 3 days at 150 °C, respectively. Formation of a valley at the cathode, and a hillock at the anode resulting from current stressing in the 75  $\mu\text{m}$  thick solder joint can be clearly observed in this figure. These surface features are less obvious in the thinner 25  $\mu\text{m}$  solder joint. The presence of the valley and the hillock as shown in Fig. 6 indicated the EM did occur in the newly designed solder joints. In addition, the entire surface feature was symmetrical about the joint thickness direction, which confirms the symmetry of the current density distribution as predicted by the simulated FEA results.

The depth of valley and height of hillock were further investigated quantitatively using a confocal laser scanning microscope. Figure 7a and c show the height map of joints investigated by CLSM, while Fig. 7b and d show the side-view of corresponding integrated height profile across the entire region of a and c respectively. From the FEA of current density distribution, it is known that there are two regions of interest: (1) center region where current densities are relatively uniform; (2) corner region with large current density gradients. These two regions are clearly apparent in Fig. 7c. At the corner regions, the valley is deeper, and the hillock is taller. It is also worth noting that valley appears to be deeper than the height of hillock, as can be seen in Fig. 7d. Further studies addressing basic issues contributing for observed features are currently underway and will be provided in future publications.

To further confirm the effects of large current density gradients, current stressed specimens were polished and examined by OM. These optical micrographs are provided in Fig. 8a and b. From the FEA simulation, the current density gradient at the corner regions becomes larger with increases in joint thickness. With a larger current density gradient, a larger compressive stress can build-up within the solder region near the cathode. This would induce a concentration gradient of vacancies from the compressive side (center of solder) to the tensile side (corner) [1], causing the vacancies to diffuse towards the corner. Voids



**Fig. 5** Optical micrographs showing the as-soldered PbSn joints with the thickness of 25  $\mu\text{m}$  (a), and 75  $\mu\text{m}$  (b)

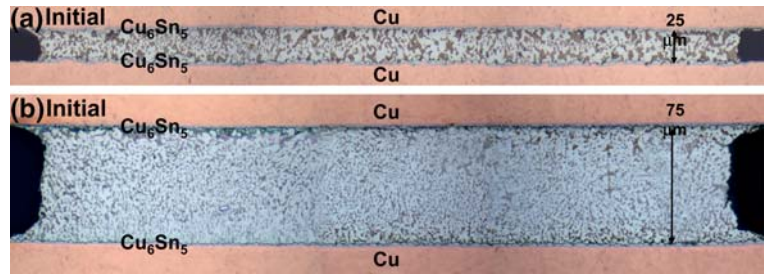


**Fig. 6** Secondary electron images showing the PbSn joints that had been aged at 150 °C for 3 days under  $10^4$  Amp/cm<sup>2</sup>: (a) 25  $\mu\text{m}$  thick joint; (b) 75  $\mu\text{m}$  thick joint. Figure b is tilted by 45° for showing the contrast of valley/hillock more clearly. The surface morphology of the dotted area is further investigated using a confocal laser scanning microscope

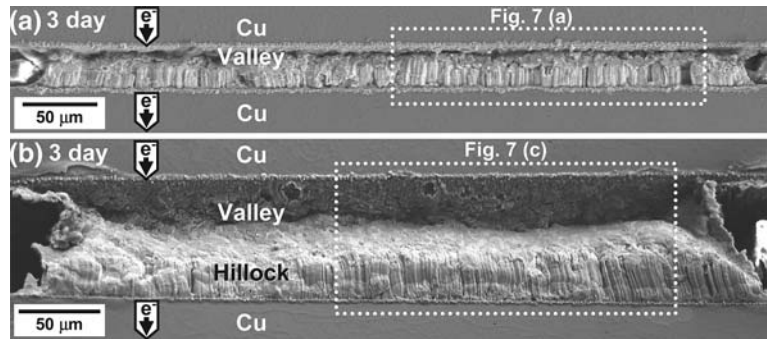
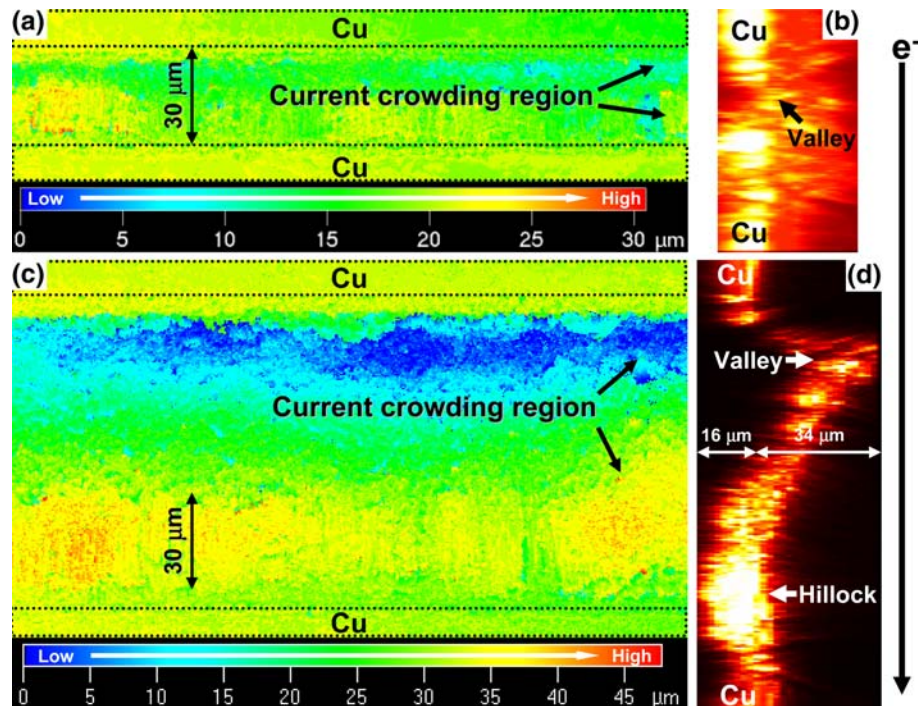


**Fig. 7** Confocal laser scanning microscopy (CLSM) showing the surface contour of the solder joints in Fig. 6: (a) 25  $\mu\text{m}$  thick joint; (c) 75  $\mu\text{m}$  thick joint. Figure (b) and (d) were the integrated side-view of (a) and (c), respectively



will form when supersaturation of vacancy is reached. Optical micrographs shown in Fig. 8a and b justify the above statement.

**4 Conclusions**

For a fundamental study to understand the important issues relating to the effects of EM on solder joint reliability, roles

of influencing factors other than imposed electric current should be minimized. The advantages of the newly developed solder joint configuration to achieve this goal include:

1. The geometry of the solder joint is symmetrical.
2. This symmetrical joint contains two regions: (1) current crowding region, and (2) relatively uniform current density region. The extent of each can be

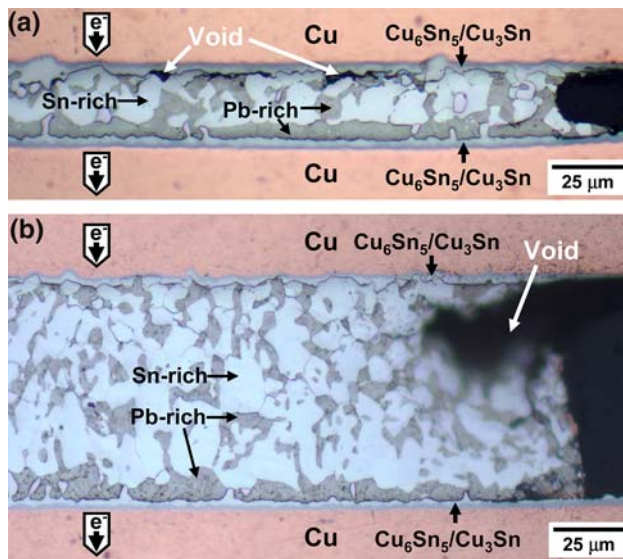


**Fig. 8** Optical micrographs showing the corner region of the PbSn joints that had been applied a  $10^4$  Amp/cm<sup>2</sup> current stressing under 150 °C for 3 days, and then polished

controlled by appropriate minor modifications in the ratio of dimensions.

3. Ease of monitoring the temperature distribution and the damage accumulation from EM.
4. No serious Joule heating (due to Cu, pillars and substrate, has an excellent thermal conductivity.).
5. No thermal gradient from the cathode to anode of the joint, preventing the influence of thermal migration.

6. Easy to adjust the size of the joint, i.e. the thickness and the diameter is adjustable.
7. Easy to change the combination of the solder joint, i.e. the composition of the solder and the base metal is adjustable.

**Acknowledgement** This project is partly supported by Hybrid-plastics, Inc. through NSF-STTR DMI-0521940.

## References

1. K.N. Tu, *J. Appl. Phys.* **94**, 5451 (2003)
2. E.C.C. Yeh, W.J. Choi, K.N. Tu, P. Elenius, H. Balkan, *Appl. Phys. Lett.* **80**, 580 (2002)
3. L. Zhang, S. Ou, J. Huang, K.N. Tu, S. Gee, L. Nguyen, *Appl. Phys. Lett.* **88**, 012106–1 (2006)
4. H. Ye, C. Basaran, D. Hopkins, *Appl. Phys. Lett.* **82**, 1045 (2003)
5. Y.H. Lin, Y.C. Hu, C.M. Tsai, C.R. Kao, K.N. Tu, *Acta Materialia* **53**, 2029 (2005)
6. S.W. Liang, Y.W. Chang, C. Chen, Y.C. Liu, K.H. Chen, S.H. Lin, *J. Electron. Mater.* **35**, 1647 (2006)
7. S.H. Chiu, T.L. Shao, C. Chen, D.J. Yao, C.Y. Hsu, *Appl. Phys. Lett.* **88**, 022110–1 (2006)
8. S.W. Liang, Y.W. Chang, C. Chen, *Appl. Phys. Lett.* **88**, 172108–1 (2006)
9. C.E. Ho, S.C. Yang, C.R. Kao, *J. Mater. Sci.–Mater. El.* **18**, 155 (2007)
10. J.W. Nah, J.O. Suh, K.N. Tu, V.S. Rao, S.W. Yoon, V. Kripesh, *TMS Annual Meeting Report*, (2006)
11. J. Kloeser, E.A. Weißbach, *Global SMT & Packaging*, p. 28 May, 2006